

# Constraining ultra light fermionic dark matter with Milky Way observations

---

**Juan Barranco**

*Departamento de Física, División de Ciencias e Ingeniería, Campus León,  
Universidad de Guanajuato, León 37150, México*

**Argelia Bernal**

*Departamento de Física, División de Ciencias e Ingeniería, Campus León,  
Universidad de Guanajuato, León 37150, México*

**David Delepine**

*Departamento de Física, División de Ciencias e Ingeniería, Campus León,  
Universidad de Guanajuato, León 37150, México*

**ABSTRACT:** The equation of state for a degenerate gas of fermions at zero temperature in the non relativistic case is a polytrope, i.e.  $p = \gamma\rho^{5/3}/m_F^{8/3}$ . If dark matter is modelled by such non interacting fermion, this dependence in the mass of the fermion  $m_F$  explains why if dark matter is very heavy the effective pressure of dark matter is negligible. Nevertheless, if the mass of the dark matter is very small, the effective pressure can be very large, and thus, a system of self-gravitating fermions can be formed. In this work we model the dark matter halo of the Milky-Way by solving the Tolman-Oppenheimer-Volkoff equations, with the equation of state for a partially degenerate ultralight non interacting fermion. It is found that in order to fit its rotational velocity curve of the Milky Way, the mass of the fermion should be in the range  $29 \text{ eV} < m_F < 33 \text{ eV}$ . Moreover, the central density is constrained to be in the range of  $46 < \rho_0 < 61 \text{ GeV/cm}^3$ . The fermionic dark matter halo has a very different profile as compared with the standard Navarro-Frenk-White profile, thus, the possible indirect signals for annihilating dark matter may change by orders of magnitude. We found bounds for the annihilation cross section in this case by using the Sagittarius A\* spectral energy distribution. Those limits are very strong confirming the idea that the lighter the dark matter particle is, the darkest it becomes.

**KEYWORDS:** Dark Matter.

---

## Contents

<b>1. Introduction</b>	<b>1</b>
<b>2. Non-interacting fermionic dark matter halo</b>	<b>3</b>
<b>3. Milky way constraints</b>	<b>8</b>
3.1 Fermion mass constraints from rotational velocity curve	9
3.2 Annihilating cross section constraints from Sgr A* data	12
<b>4. Conclusions</b>	<b>14</b>

---

## 1. Introduction

The determination of the properties of the particle that play the role of dark matter is perhaps the most active field in experimental and theoretical physics of our time [1, 2, 3, 4]. In spite of this effort, up to now, none of the properties of dark matter are known. Not even its mass or its spin. Taking into account only this two properties, the mass and the spin of the dark matter candidate, we can divide many models and candidates for dark matter in at least three main streams:

1. the heavy mass fermionic (spin one-half) candidate, i.e. the weakly interacting massive particle (WIMP) [5],
2. the ultra-light massive spin zero particle candidate, i.e. the axion-like particles [6, 7, 8, 9, 10, 11, 12, 13, 14, 15, 16] and,
3. the ultra-light fermionic dark matter candidate, i.e. the sterile neutrino [17, 18, 19, 20, 21]

The WIMP paradigm is strongly motivated by the elegant thermal freeze-out mechanism for dark matter production [5]. Among the many WIMP candidates, the prototype of a WIMP particle is the neutralino, and other supersymmetric candidates [3]. Actually, the WIMP fits perfectly in the standard cosmological model because they are massive enough to be "cold relics". That means that they decoupled after they became non-relativistic. Astrophysical observations need in addition to Cold dark matter (CDM), a cosmological constant  $\Lambda$  in order to explain the present accelerated expansion of the universe. This is the so called  $\Lambda$ -CDM model. Among their

virtues, N-body simulations within a  $\Lambda$ -CDM universe fit most of the cosmological observables like Supernova Ia data, the power spectrum, weak lensing and more [22]. Furthermore, it has some predictions: a universal density profile from hierarchical clustering for the dark matter halo of galaxies, commonly referred as the Navarro-Frenk-White (NFW) dark matter profile [23]. This profile has central densities that rises as  $\rho \sim r^{-\beta}$ , with  $\beta \sim 1 - 1.5$ . Nevertheless, observed galaxy rotation curves favor a constant density profile. This is known as the "*Core-Cusp*" problem [24]. Moreover, the number of predicted satellite galaxies is bigger than the observed. This problem is known as the "*missing satellite problem*" [25]. Another problem rises from N-body simulations: the average density of dwarf galaxies is much bigger than the observed densities of the local group, a problem that is known as the *Too big to fail* problem [26]. More troubles arise as soon as current experimental efforts have not reveal any positive signal of their existence. Neither by direct detection experiments [27] or by indirect detection [1] in any of different possible astrophysical signatures. Furthermore, DM collider production has not been observed yet [28].

In order to solve some of the galactic puzzles at small scales that permeates the WIMP paradigm, new proposals like fuzzy dark matter 2) and sterile neutrinos 3) have been introduced. Indeed, a plethora of ultra-light scalar candidates with properties similar to that of the axion have been postulated, called axion-like dark matter particles, fuzzy dark matter or simply Scalar Field dark matter [6, 7, 8, 9, 10, 11, 12, 13]. Those are zero spin particles with masses ranging from  $10^{-23}$  to  $10^{-3}$  eV. Originally, the axion was proposed as a dynamical solution for the strong CP problem [6, 7, 8]. It was soon realized that it could be a perfect dark matter candidate [29] and for the last 40 years its mass and decay constant have been constrained. Surprisingly, it is still a viable candidate [4].

In a different approach, an ultra-light scalar particle,  $m \sim 10^{-23}$  eV, minimally coupled to gravity without any interaction with the standard model of particles was proposed as a viable dark matter candidate [9, 10, 11]. One virtue of this proposal is the emergence of a natural cut-off in the power spectrum [10]. Thus, no small halos exist in SFDM solving the "*missing satellite*" problem. Furthermore, in these models, the halos are modelled by the self-gravitating system made of ultra-light scalar fields. In the particular case of complex scalar fields, those structures are the so called Boson Stars (BS). For a scalar field mass of the order  $m \sim 10^{-23}$  eV, the resulting BS have typical masses of  $M \sim 10^{11} M_{\odot}$  and their radii are of several kiloparsecs, making these boson stars suitable dark matter halo models [14, 15]. Furthermore, BS are regular at  $r = 0$  and thus, there is no "*core-cusp*" problem [16]. In other words, ultra light bosonic particles might be free of some of the  $\Lambda$ -CDM problems.

This motivates a revival on axion-like dark matter candidates, that is, particles that have some interaction with SM particles similar to the axion, although not necessarily related with the strong CP problem, and with extreme low mass values, i.e.  $m \sim 10^{-23} - 10^{-15}$  eV [12, 13].

Then we arrive to the case of ultra-light fermionic dark matter, i.e. a particles with 1/2 spin and masses between  $\sim 1$  eV to 10 keV usually called sterile neutrinos [20, 18, 21, 17, 19]. Those DM candidates were advocated to improve predictions of small scale structure [21]. The strongest constraints on sterile neutrino come from the Planck measurement on the number of relativistic species in the early universe,  $N_{eff}$ , recently measured by the Planck collaboration [30]. Those constraints can be evaded introducing a non standard relic density production mechanism [18, 21]. The purpose of this work is to study the properties that dark matter halos would have if dark matter is an ultra-light semi-degenerate fermion with negligible interaction. Similar analysis had been done in [31, 32, 33, 34]. There are three main differences in comparison with those works and the present: i) we study for the first time the Milky Way rotational curve data in order to constraint the mass of the fermions, ii) the gas of fermions is treated as a semi-degenerate gas, and thus, we can apply the formalism to big galaxies and iii) we obtain constraints on the annihilation cross section from the spectral energy distribution of the central black hole of the Milky way.

Typical self-gravitating objects made of ultra light fermions are presented in section 2. Then, by using galactic observations. namely the rotational velocity curve of the Milky Way as reported by [35], the central density  $\rho_0$  and the mass of the fermion  $m_F$  are constrained in section 3. Furthermore, by using the spectral energy distribution (SED) of Saggitarius A\* observed from the galactic centre, new constraints on the annihilating cross section are obtained. Finally, some conclusions can be found in section 4.

## 2. Non-interacting fermionic dark matter halo

A gas of fermions is degenerate at temperatures

$$T < T_{Deg} = \frac{2\pi\hbar^2}{m_f K_B} \left( \frac{\rho}{2m_f} \right)^{2/3}, \quad (2.1)$$

where  $m_f$  is the mass of the Fermion,  $\rho$  the mass density of the fermion gas, and  $K_B$  the Boltzmann constant. The mass density and pressure for a degenerate gas of fermions can be computed as [36, 37]

$$\begin{aligned} p &= \frac{m_F^4}{24\pi^2} [(2z^3 - 3z)(1+z)^{1/2} + 3\sinh^{-1}(z)], \\ \rho &= \frac{m_F^4}{8\pi^2} [(2z^3 + z)(1+z)^{1/2} - \sinh^{-1}(z)]. \end{aligned} \quad (2.2)$$

where  $z = \frac{K_F}{m_F}$ ,  $K_F$  the Fermi momentum.

There are two interesting limits, the non-relativistic case where  $z \ll 1$  (i.e. the mass of the fermion is too big as compared with the Fermi momentum) and the

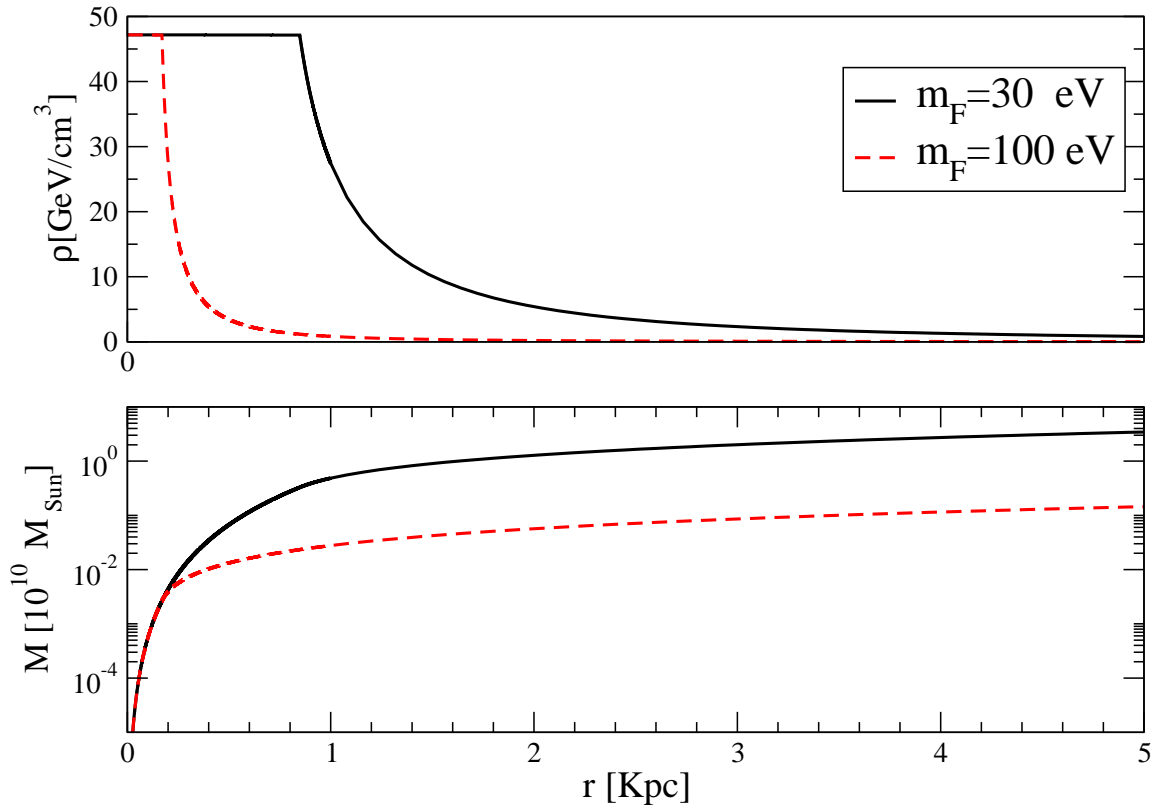


**Figure 1:** Self-gravitating structures made of non-interacting, non-relativistic semi-degenerate fermions at zero temperature. In the upper panel it is shown typical density and mass profiles for a central density of  $\rho_0 = 47 \text{ GeV/cm}^3$  for two different masses of the fermion, namely  $m_F = 30 \text{ eV}$  (solid) and  $m_F = 100 \text{ eV}$  (dashed). The flat central region of the density profile correspond to the degenerate gas. Lower panel shows the mass function.

relativistic limit  $z \gg 1$ . In the non-relativistic case, by doing an expansion for  $z \ll 1$  in eqs. 2.2 it is found that the pressure can be written as a function of the density. Indeed, it is found that

$$p = \frac{34}{65} \left( \frac{6\pi^2}{13} \right)^{2/3} \frac{\rho^{5/3}}{m_F^{8/3}}. \quad (2.3)$$

Meanwhile, in the relativistic case, it is found

$$p = \frac{(3\pi^2)^{1/3}}{4} \frac{\rho^{4/3}}{m_F^{4/3}}. \quad (2.4)$$

It is interesting to note that the resulting equation of state for a gas of degenerate fermions is a polytrope, and it has only one free parameter: the mass of the fermion.

In order to find the self-gravitating structure that a gas of free fermions may form, it is needed to solve the Einstein's equations. As we have mentioned, in the non-relativistic limit, this gas of fermions satisfies an equation of state in a very

similar way as a perfect fluid may do. Thus, the energy tensor that acts as a source for the Einstein equations can be written as:

$$T_{\mu\nu} = pg_{\mu\nu} + (p + \rho)U_\mu U_\nu. \quad (2.5)$$

Here,  $U_\mu$  is the four velocity of the fluid,  $p$  and  $\rho$  the pressure and density of the fluid.

For simplicity, we will restrict to the case of spherical symmetry and static space-time, that is, the Schwarzschild metric. Spherical symmetry is well justified by observational evidence that implies that the shape of the Milky Way dark matter halo is nearly spherically symmetrical [38]. In this case, the only unknown in the metric is the mass of the self-gravitating object. Imposing the condition of hydrostatic equilibrium one arrives to the following equations

$$\begin{aligned} \frac{dp}{dr} &= -\frac{GM\rho}{r^2} \left(1 + \frac{p}{\rho}\right) \left(1 + \frac{4\pi r^3 p}{M}\right) \left(1 - \frac{2GM}{r}\right)^{-1}, \\ \frac{dM}{dr} &= 4\pi r^2 \rho. \end{aligned} \quad (2.6)$$

Those are the Tolman-Oppenheimer-Volkoff equations (TOV system).

If the self-gravitating configurations have low compactness, that is  $GM/r \ll 1$ , thus, the TOV system is rewritten in the limit of low compactness as:

$$\frac{dp}{dr} = -\frac{GM\rho}{r^2}, \quad (2.7)$$

$$\frac{dM}{dr} = 4\pi r^2 \rho. \quad (2.8)$$

This is known as the Newtonian limit of the TOV system.

The system can be solved once the equation of state (EOS) of the fluid is known. In the case of degenerate fermions, the corresponding EOS will be given by eq. 2.3. Nevertheless, it could happen that at some point the temperature of the gas of fermions can be bigger than  $T_{Deg}$ . The temperature at any point of the gas can be determined using the virial theorem:

$$T = \frac{GMm_F}{K_B r}, \quad (2.9)$$

where  $K_B$  is the Boltzmann constant,  $M$  is the enclosed mass of the compact object, and  $r$  the radial distance where the temperature is computed. If  $T > T_{Deg}$  eq. 2.3 is not valid anymore since it is valid only for a fully degenerate gas of fermions. Instead, the classical pressure will be used and it is given by:

$$P(\rho) = \frac{GM\rho}{2r}. \quad (2.10)$$

With those considerations, depending on the temperature of the fermion, the equation of state will be either the eq. 2.3 if the gas of fermions has a temperature below  $T_{Deg}$  or equation of state eq. 2.10 if  $T > T_{Deg}$ .

Consequently, the Newtonian TOV system we need to solve will depend on the corresponding temperature. If  $T < T_{Deg}$ , eq. 2.7 reduces to

$$\frac{d\rho}{dr} = -\frac{39}{34} \left( \frac{13}{6\pi^2} \right)^{2/3} \frac{GM}{r^2} m_F^{8/3} \rho^{1/3}, \quad (2.11)$$

and if  $T > T_{Deg}$

$$\frac{d\rho}{r} = -\frac{\rho}{r} - 4\pi \frac{\rho^2 r^2}{r}. \quad (2.12)$$

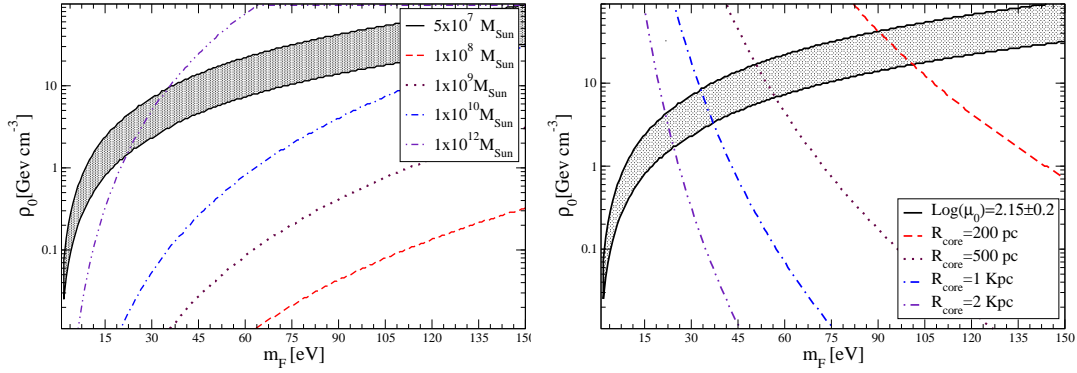


**Figure 2:** Isocurves for the full set of self-gravitating configurations obtained by varying the free parameters  $m_F$  and  $\rho_0$ . Left panel: The total mass  $M(\rho_0, m_F)$ . Right panel: the core radius  $R_{core}(\rho_0, m_F)$ . The allowed region for  $\rho_0$  and  $m_F$  needed to have configurations that fulfill the condition of constant dark matter surface density, i.e. eq. 2.15, are shown with a grey band in both panels.

The equations 2.8 and 2.11 can be solved numerically, with boundary conditions  $M(r=0) = 0$  and  $\rho(r=0) = \rho_0$ ,  $\rho_0$  a free parameter. Integration of equations 2.8 and 2.11 is performed until the point  $T = T_{Deg}$ . The radius  $R_{core}$  where  $T = T_{Deg}$  fixes the core of the configuration. At this point the mass contained will be denoted as  $M_* = M(R_{core})$  and it will correspond to a fixed mass density  $\rho_* = \rho(R_{core})$ . It can be shown that for  $T > T_{Deg}$ , the solution of equations 2.8 and 2.12 with boundary conditions  $M(r = R_{core}) = M_*$  and  $\rho(r = R_{core}) = \rho_*$  are:

$$\rho(r) = \frac{\rho_* M_* R_{core}}{r \sqrt{4\pi \rho_* M_* R_{core} (r^2 - R_{core}^2) + M_*^2}} \quad (2.13)$$

and

$$M(r) = \sqrt{4\pi \rho_* M_* R_{core} (r^2 - R_{core}^2) + M_*^2} \quad (2.14)$$

Note that the mass density  $\rho(r)$  decays as  $r^{-2}$  and the mass goes as  $M(r) \sim r$ . The mass of the configuration is always a growing function of  $r$  and the compact

structure does not have a finite radius. Nevertheless, since  $\rho(r)$  is a decreasing function for all  $r$ , we can define the radius of the self-gravitating object as the point where  $\rho(r = R) < \rho_c$ , with  $\rho_c$  the critical density of the universe.

The value of  $R_{core}$  where  $T = T_{Deg}$  is determined by  $\rho_0$ . Then, the self-gravitating system have only two free parameters:

- The mass of the dark matter fermion  $m_F$  and,
- the central density of the configuration  $\rho_0$ .

Typical configurations will have a density profile and a metric coefficient  $M(r)$  as shown in Fig. 1. For definitiveness, two different values of the mass of the fermion are shown, namely,  $m_F = 30$  eV and  $m_F = 100$  eV for central density of  $\rho_0 = 47$  GeV/cm<sup>3</sup>. Note that the masses of the self gravitating objects are of the order of  $M \sim 10^{11} M_\odot$  and radii of  $R \sim 10$  kpc for those values of the fermion mass. Thus it is clear that this self-gravitating structures made of semi-degenerate fermions might play the role for cored dark matter halos. In what follows, we will say that the dark matter particle candidate is such non interaction fermion with ultralight values of the mass ( $\sim$  few electronVolts).

In order to see the properties of the dark matter halos made of a gas of semi-degenerate ultralight fermions, we have constructed the full set of solutions of equations 2.8 -2.12 obtained by varying the two free parameters of the dark matter halo: the central density  $\rho_0$  and the mass of the fermion  $m_F$ .

In Fig. 2 are shown iso-curves of the total mass  $M(m_F, \rho_0)$  and in the right panel are shown iso-curves of the core radius  $R_{core}(m_F, \rho_0)$ .

We can observe that for low central densities, the resulting configurations have properties that might explain dwarf galaxies data: core radius of the order of hundred parsecs and masses of the order of  $\sim 10^8 M_\odot$  for values of the fermion mass of  $m_F \sim 100$  eV.

On the other hand, for smaller masses of the fermions, the configurations might be suitable to explain larger galaxies, like elliptical or espiral galaxies because the resulting core radius are the order of few kiloparsecs, rotational velocities of hundreds of  $km/sec$  and total masses of  $10^{11} M_\odot$  for masses of the fermion of tens of eV. This is a consequence of the fact that the pressure of the fermion gas is inverse proportionality to the mass  $m_F$ .

The so called  $\Lambda$ -CDM model describe the large scale structure of the universe. Nevertheless, as previously mentioned, the  $\Lambda$ -CDM predictions at low scales are in debate [50]. In particular, the "core-cusp problem" [24] and the "too big to fail" [26] problems can be solved by invoking new interactions in the dark sector. Indeed, if dark matter has strong self-interactions, elastic scattering in the dense central region of halos will redistribute the energy and angular momentum among particles creating a core [51]. Other solutions rely on supernova feedback and low



Region (R)	Central density $\rho_R^c$ [ $10^{10} M_\odot \text{kpc}^{-3}$ ]	Scale radius $a_R$ [kpc]
Inner Bulge (IB)	$\rho_{IB}^c = 3.6 \times 10^3$	$a_{IB} = 3.8 \times 10^{-3}$
Main Bulge (MB)	$\rho_{MB}^c = 19.0$	$a_{MB} = 1.2 \times 10^{-1}$
Disk (D)	$\rho_D^c = 1.50$	$a_D = 1.2$

**Table 1:** Values used to fit the inner region of the milky Way’s rotational velocity curve

star-formation efficiency. The first one might flatten the central cusp in big galaxies and a combination of both could explain why most of the Milky Way’s dark matter subhalos do not host visible galaxies [52].

It is interesting that in our case, even without the addition of any other interaction in the dark sector, the resulting self-gravitating configurations might alleviate some of the  $\Lambda$ -CDM problems: There is no core-cusp problem since the dark matter halos have naturally a core  $R_{core}$  produced by the degenerate gas. Furthermore, here there is not a Too big to fail problem since the central density  $\rho_0$  is smaller than the central densities needed by NFW dark matter halos.

Finally, there are some interesting scaling relations found empirically for the dark matter halos. In particular, in [53, 54] it was found that the central surface density of galaxy dark matter haloes defined as  $\mu_{0D} = R_{core}\rho_0$ , where  $R_{core}$  and  $\rho_0$  are the halo core radius and central density respectively, is nearly constant. It was found

$$\log\left(\frac{\mu_{0D}}{M_\odot \text{pc}^{-2}}\right) = 2.15 \pm 0.2 \quad (2.15)$$

and independent of galaxy luminosity.

From all possible configurations for dark matter haloes made of semi-degenerate fermions, there is a subset that can full fill that relation between core radius and central density.

Those configurations defined a region in the  $(\rho_0, m_F)$  parameter space that satisfies the condition eq. 2.15. This region is shown in the two panels of Fig. 2 as a grey band. Notice that this condition is fulfilled by a small fraction of the total possible self-gravitating configurations. We will show that if the Milky Way dark matter halo is made of ultralight fermions, the resulting configuration do not satisfy eq. 2.15.

### 3. Milky way constraints

From our results of the previous section, we observe that self-gravitating configurations for non interacting fermions cover a wide range of masses and core radii. Thus, they can be used to model different types of galaxies. From the smallest dwarf galaxies with  $M \sim 10^7 M_\odot$  and core radius of a hundreds of parsecs up to spiral galaxies with  $M \sim 10^{11} M_\odot$  and core radius of few kiloparsecs.

In this section we will use data from our own galaxy in order to see if this very simple model might fit the observed data. In contrast with other galaxies, our Milky Way is perhaps one of the best known galaxy. We will constraint the mass of the fermion  $m_F$  and the central density  $\rho_0$  with the rotational velocity of the stars in our galaxy. Then, we will constraint the annihilation cross section for this ultra light

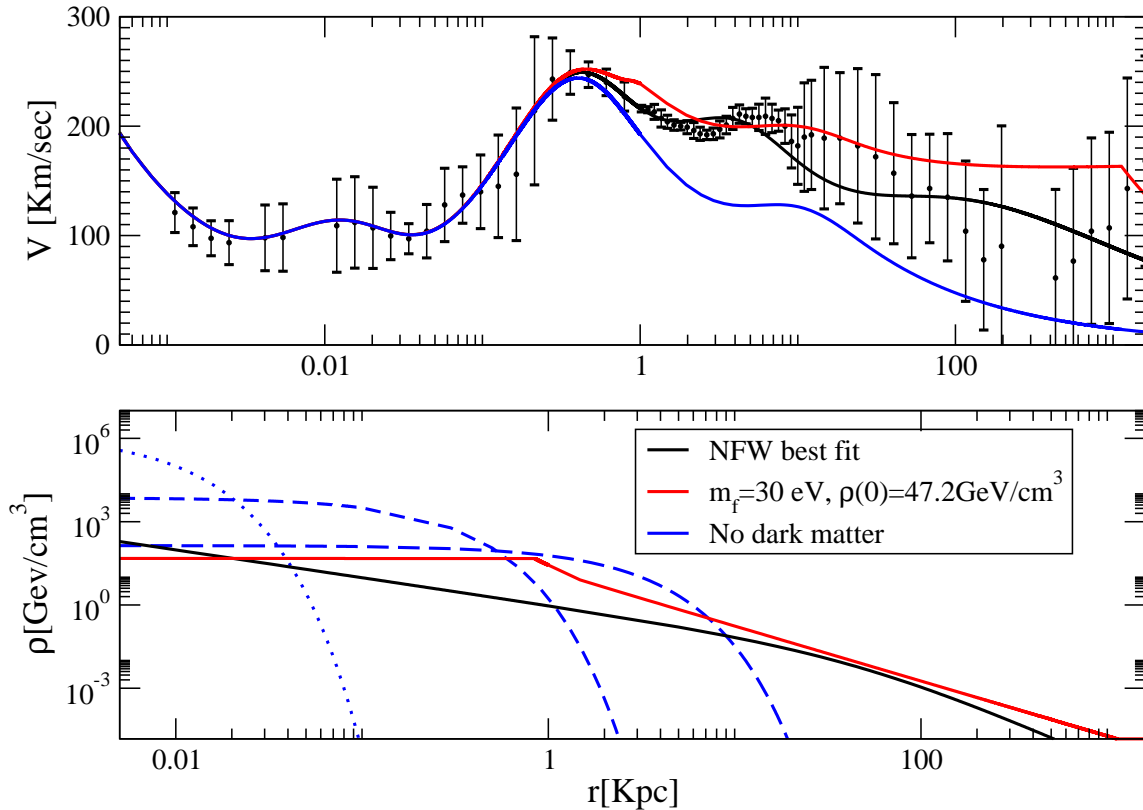


**Figure 3:** Milky way rotational velocities and theoretical rotational curve obtained for the best fit  $\rho_0 = 47 \text{ GeV cm}^{-3}$ ,  $m_F = 30 \text{ eV}$  for a dark matter halo model made of semi-degenerate non-interacting fermions )

Recent observation in the CO and CS line emissions from the central region of the galaxy have been used to derive the central rotational curve of the Milky way. This rotational curve covers a wide range of radius, from  $\sim 1\text{pc}$  up to several hundred kpc [35]. The inner rotational curve can be fitted if Milky Way is divided in five different components:

1. The central black hole
2. A inner bulge or core of the galaxy

3. The main bulge
4. The disk of the galaxy
5. A dark matter halo

Each component can be modelled if the mass density is described by an exponential sphere model. In this case, the mass density profile  $\rho(r)$  is given by:

$$\rho_R(r) = \rho_R^c \exp(-r/a_R), \quad (3.1)$$

$a_R$  being a scale radius,  $\rho_R^c$  the central density for each region, and  $R$  a label to identify each of the regions that fits the milky way. The dark matter halo will be modelled by the self-gravitating structure of semi-degenerate fermions.

The values used in order to fit the rotational curve are shown in Table 1. The existence of a supermassive black hole at the center of our galaxy is strongly supported by the motion of the S-star galaxies. Its mass has been constrained to be  $M_{BH} = (4.1 \pm 0.6) \times 10^6 M_\odot$  [39].

The theoretical velocity curve can be computed as

$$v^{th}(r) = \sqrt{\sum_{R=IB,MB,D} v_R^2(r) + v_{BH}^2(r) + v_{DM}^2(r)} \quad (3.2)$$

where

$$\begin{aligned} v_{BH}(r) &= \sqrt{G \frac{M_{BH}}{r}} \\ v_R(r) &= \sqrt{\frac{GM_R}{r}}, R = IB, MB, D \\ v_{DM}(r) &= \sqrt{\frac{GM_{DM}}{r}}. \end{aligned} \quad (3.3)$$

$M_R(r)$  is computed by integration of the mass density as defined by eq. 3.1, i.e:

$$M_R(r) = 8\pi a_R^3 \rho_R^c (1 - e^{-r/a_R}) \left( 1 + \frac{r}{a_R} + \frac{1}{2} \left( \frac{r}{a_R} \right)^2 \right). \quad (3.4)$$

Finally, the mass of the black dark matter halo is computed by solving the TOV system eqs. 2.8 and 2.11 for  $T < T_{Deg}$  and eqs. 2.8-2.12 for  $T > T_{Deg}$ . Remember that the only unknowns in the solution of the TOV equations are the central density  $\rho_0$  and the mass of the fermion  $m_F$ . In other words,  $M_{DM} = M_{DM}(\rho_0, m_F)$ . Then, the rotational velocity will depend on the choice of the dark matter central density and the mass of the fermion.

As we have already mentioned, the rotational curve of the Milky Way has been derived for a huge range of values, ranging from pc to kpc. The values are reported

in [35]. The inner region is dominated by the luminous matter. In Fig. 3 we have plotted the theoretical rotational velocity curve for different scenarios: First, by neglecting the contribution of the dark matter halo, we can see that with the values reported in Table 1, the inner part of the rotational curve is well fitted, the inner part does not need a major contribution of dark matter. The resulting rotational velocity curve without DM is shown as a blue curve in the upper panel of Fig. 3. This rotational curve arises from the effect of the matter of the BH, the inner and main bulge and the disk. Their corresponding contribution to the mass density is shown in blue lines in the lower panel of Fig. 3. Nevertheless, the outer part needs the contribution of dark matter. We then consider a second scenario: the full rotational velocity curve can be fitted with the inclusion of a dark matter halo that in this case will be modelled by the self gravitating structure formed by a gas of non-interacting fermions with equation of state given by eq. 2.3 in hydrostatic equilibrium with gravity. The solution for the mass function and the density depend on the central density  $\rho_0$  and the mass of the fermion  $m_F$ , then,  $v^{th}(r_i) = v^{th}(r_i, \rho_0, m_F)$ ,  $r_i$  is the value of the radial coordinate where it has been reported the observed rotational velocity as reported by [35]. In order to find the value of the fermion mass and the central density of dark matter needed to fit the observed rotational curve, we have performed a  $\chi^2$  analysis given by:

$$\chi^2(\rho_0, m_F) = \sum_{i=1}^{67} \left( \frac{v^{th}(r_i, \rho_0, m_F) - v_i^{Obs}}{\delta v_i^{obs}} \right)^2. \quad (3.5)$$

where  $v_i^{Obs}$  and  $\delta v_i^{obs}$  are the observed values of the rotational velocity curve and the corresponding error as reported in [35].

Isocurves of  $\Delta\chi^2 = \chi^2(\rho_0, m_F) - \chi_{min}^2$  are shown in Fig. 4. In particular, we shown isocurves for  $\Delta\chi^2 = 2.71$ ,  $\Delta\chi^2 = 4.61$  and  $\Delta\chi^2 = 5.99$ , that represent the allowed values for  $m_F$  and  $\rho_0$  that fits within  $1\sigma$  (68% C.L.), 90% C.L. and 95% C.L. respectively. Thus, at  $1\sigma$ , the best fit point that fits the milky way rotational velocity curve are:

$$\rho_0 = 47_{-1}^{+14} \text{ GeV/cm}^3 \quad (3.6)$$

$$m_F = 30_{-1}^{+3} \text{ eV}. \quad (3.7)$$

The resulting dark matter density profile for the Milky Way is shown as a red line in the lower panel of Fig. 3 and the resulting rotational velocity curve that includes the luminous matter and the DM contribution is shown in upper panel of Fig. 3 with a red line too. In order to show the differences with the standard dark matter profile and the one it is obtained with ultra light non interacting fermions, for comparison, we have included the best fit for a Navarro-Frenk-White density profile as a black line in both figures. Observe that the central density of the NFW dark matter halo is bigger than the corresponding central density of a semi-degenerate gas of fermions.

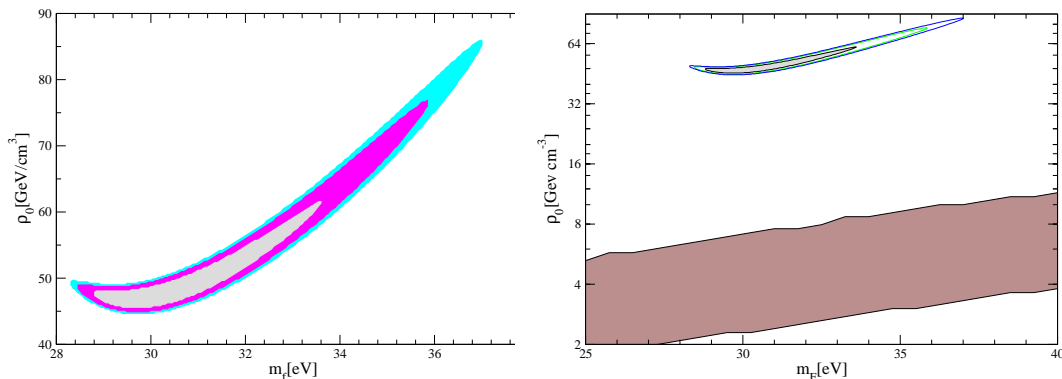


**Figure 4:** Left: Isocurves at 68% C.L and 95% C.L. for the mass of the fermion and central densities that fit the Milky Way rotational curve data. The dot corresponds to the best fit point. Right: The allowed region in the parameter space  $(m_F, \rho_0)$  that adjust the rotational curve of the Milky Way. In marron it is shown the region in  $(m_F, \rho_0)$  that fulfills eq. 2.15.

The bounds obtained for  $\rho_0, m_F$  with the fit to the rotational curve of the Milky Way can be complemented with other observables. In particular, similar approaches for ultralight fermionic dark matter have been used to fit data from dwarf galaxies. In [34], it is found that a fermion with  $70 < m_F < 500$  eV can fit the data of the dispersion velocities of the dwarf satellite galaxies of the Milky Way. Furthermore, as we have mentioned, there is a region in the  $(m_F, \rho_0)$  parameter space where the relation of a constant surface dark matter halo, i.e. eq. 2.15, is fulfilled. As it can be noted in order to find if the values needed to satisfy both the Milky Way rotational curve data and the dispersion velocities of Dwarf galaxies, a combined analysis must be done and considering in both cases a semi-degenerate gas of fermions.

We finish this section by pointing out that in this case, the dark matter halo made of semi-degenerate fermions does not full fill eq. 2.15. This is shown in the right panel of Fig. 4, where we plot the allowed region for  $(m_F, \rho_0)$  that fits the rotational curve of the Milky Way and the values of  $m_F$  and  $\rho_0$  that satisfies the constant density surface of the galaxies observed in [53, 54]. As we can see, both regions are incompatible.

### 3.2 Annihilating cross section constraints from Sgr A\* data

In this section we will use the spectral energy distribution observed from the center of the Milky Way in order to constrain the possible annihilating cross section of this ultra-light fermion. This source of radio is known as Sagittarius A\*.

Sagittarius A\* (Sgr A\*) is a compact radio source at the Galactic Center. Sgr A\* is frequently monitored at all available wavelengths. First data in radio was taken in the middle 70's [43] and from that moment up to now, Sgr A\* is observed in radio as reported recently in [44, 45]. There is also available data recorded in submillimeter,

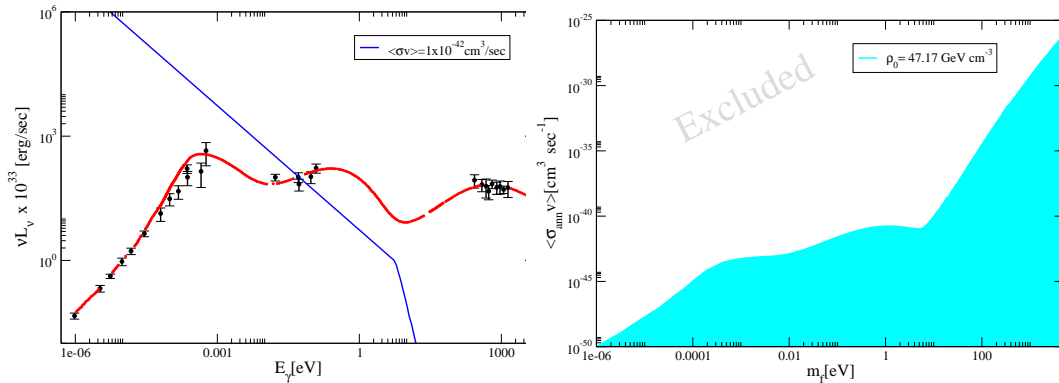


**Figure 5:** Left: Luminosity from the galactic center. In red a model of the luminosity [49] and in blue the possible contribution to the spectral energy distribution of SgrA\* in case that the dark matter of the Milky way halo is made of annihilating dark matter ultralight fermions. That excess in the SED will correspond to a halo with central density  $\rho_0 = 47 \text{ GeV/cm}^3$  and a average  $\langle\sigma v\rangle = 10^{-42} \text{ cm}^3/\text{sec}$ . Right: Annihilation cross section needed to avoid an excess in the observed SgrA\* spectrum energy distribution

near-infrared (NIR), and X-rays [46, 47, 48]. In addition to observations done in the electromagnetic spectrum, there are stellar dynamical data of the stars at the galactic center that in conjunction with the spectral energy distribution (SED) suggest that Sgr A\* is a supermassive black hole. Sgr A\*'s SED can be fit with semianalytical models [49] and it is a intense source of research. For definitiveness, in Fig. 5 we report the data and in red a model for the SED of SgrA\* as reported in [49] that we will use in order to constraint possible contributions of annihilating ultra light dark matter.

We have shown that the dark matter halo of the Milky Way can be modelled by the self-gravitating configurations made of ultralight semi-degenerate fermions. Under the hypothesis that such fermions might annihilate themselves, there will be a extra contribution in the SED of SrgA\*. Indeed, there will be a local flux of extra photons coming from the galactic center for annihilating dark matter. This flux is given by:

$$\phi_\gamma = \frac{1}{4\pi} \frac{N_\gamma E_\gamma}{2m_F^2} \int \sigma v(r) \rho^2(r) dV. \quad (3.8)$$

where  $m_F$  is the particle mass,  $N_\gamma$  is the number of photons per interaction,  $E_\gamma$  is the photon energy,  $\sigma$  is the interaction cross section,  $v(r)$  is the velocity distribution of the dark matter as a function of radius and the integral is over the observed volume. We assume two photons with  $E_\gamma = m_F$  per annihilation and that  $v$  is independent of radius. As an example of this possible photon excess in the Saggi-tarius A\* spectra energy distribution, we have computed the dark matter photon flux that correspond to a halo configuration made of ultra light fermions with central density  $\rho_0 = 47 \text{ GeV/cm}^3$  and an average annihilating cross section fixed as

$\langle\sigma v\rangle = 10^{-36}\text{cm}^3/\text{sec}$ . Furthermore, we have assumed that the mass of the fermion will be equal to the photon energy  $m_F = E_\gamma$ . This contribution is plotted in a blue line the left panel of Fig. 5.

We can now use the SgrA\* SED model of [49] to constraint  $\langle\sigma v\rangle$ . In order to do so, we have to found the self-gravitating structures with  $m_F = E_\gamma$  and  $\rho_0 = 47\text{Gev}/\text{cm}^3$  by solving the TOV system for the semi-degenerate system of fermions. Once computed the DM distribution  $\rho(r)$  it is possible to compute the possible extra flux of photons with eq. 3.8. The contribution to the SgrA\* SED,  $\langle\sigma v\rangle$  should be smaller than the observed SgrA\* spectrum and thus it is possible to constrain the annihilating cross section. This limit for  $\langle\sigma v\rangle$  is shown in the right panel of Fig. 5.

Due to the smallness of the dark matter fermion, the number density is very high, and then, the constraints shown in Fig. 5 are very strong. This effect of light dark matter should be general, that is, the interaction of light dark matter with SM particles should be very small, otherwise visible effects should arise immediately due to the high number density. The lightest the dark matter is, the darkest it should become.

## 4. Conclusions

We conclude that if dark matter is a ultra light, non interacting fermion, the dark matter halos should be modelled as the self gravitating structure supported by the quantum pressure of the fluid. In this scenario, halos will have a core, thus there is no "core-cusp" problem. The central densities of the halos are orders of magnitude smaller that the corresponding Navarro-Frenk-White profiles, thus lessening the "too big to fail" problem. In order to fit the rotational curve of the Milky Way, the mass of the fermion is constrained to be  $29 < m_F < 33\text{eV}$  and the central density of the halo lies within the range  $46 < \rho_0 < 61\text{GeV}/\text{cm}^3$  at 68% C.L. The resulting halo has a core radius that giving the central density does not satisfy the constant density surface restriction founded in [53, 54] (see right panel of Fig. 4).

Given the small masses of the fermions, in case that this dark matter annihilates into photons, there will be a low energy photons coming from the galactic center. This photons will contribute to the spectrum energy distribution and thus, by using the data of the Sgr A\* SED it was possible to found constraints on  $\langle\sigma v\rangle$ . Constraints are very strong, supporting the idea that this type of fermions do not have a thermic origin.

In summary, Milky Way data might provide strong constraints on models where dark matter is modelled by and ultra light fermion. Either by stellar dynamics data or by the low energy photons coming from the galactic center. Combined analysis with data from Milky Way's dwarf galaxies, structure formation can be made in order to discard this simple model of dark matter.

## Acknowledgments

This work was partially support by CONACYT project CB-259228 y CB-286651 and Conacyt-SNI.

## References

- [1] G. Arcadi, M. Dutra, P. Ghosh, M. Lindner, Y. Mambrini, M. Pierre, S. Profumo and F. S. Queiroz, *Eur. Phys. J. C* **78**, no. 3, 203 (2018)  
doi:10.1140/epjc/s10052-018-5662-y [arXiv:1703.07364 [hep-ph]].
- [2] G. Bertone, D. Hooper and J. Silk, *Phys. Rept.* **405**, 279 (2005)  
doi:10.1016/j.physrep.2004.08.031 [hep-ph/0404175].
- [3] G. Jungman, M. Kamionkowski and K. Griest, *Phys. Rept.* **267**, 195 (1996)  
doi:10.1016/0370-1573(95)00058-5 [hep-ph/9506380].
- [4] M. Tanabashi *et al.* [Particle Data Group], *Phys. Rev. D* **98**, no. 3, 030001 (2018).  
doi:10.1103/PhysRevD.98.030001
- [5] B. W. Lee and S. Weinberg, *Phys. Rev. Lett.* **39**, 165 (1977).  
doi:10.1103/PhysRevLett.39.165
- [6] S. Weinberg, *Phys. Rev. Lett.* **40**, 223 (1978). doi:10.1103/PhysRevLett.40.223
- [7] F. Wilczek, *Phys. Rev. Lett.* **40**, 279 (1978). doi:10.1103/PhysRevLett.40.279
- [8] R. D. Peccei and H. R. Quinn, *Phys. Rev. Lett.* **38**, 1440 (1977).  
doi:10.1103/PhysRevLett.38.1440
- [9] T. Matos and F. S. Guzman, *Class. Quant. Grav.* **17**, L9 (2000)  
doi:10.1088/0264-9381/17/1/102 [gr-qc/9810028].
- [10] T. Matos and L. A. Urena-Lopez, *Phys. Rev. D* **63**, 063506 (2001)  
doi:10.1103/PhysRevD.63.063506 [astro-ph/0006024].
- [11] W. Hu, R. Barkana and A. Gruzinov, *Phys. Rev. Lett.* **85**, 1158 (2000)  
doi:10.1103/PhysRevLett.85.1158 [astro-ph/0003365].
- [12] D. J. E. Marsh, *Phys. Rept.* **643**, 1 (2016) doi:10.1016/j.physrep.2016.06.005  
[arXiv:1510.07633 [astro-ph.CO]].
- [13] L. Hui, J. P. Ostriker, S. Tremaine and E. Witten, *Phys. Rev. D* **95**, no. 4, 043541 (2017) doi:10.1103/PhysRevD.95.043541 [arXiv:1610.08297 [astro-ph.CO]].
- [14] A. Bernal, J. Barranco, D. Alic and C. Palenzuela, *AIP Conf. Proc.* **1241**, 335 (2010). doi:10.1063/1.3462653
- [15] L. A. Urena-Lopez and A. Bernal, *Phys. Rev. D* **82**, 123535 (2010)  
doi:10.1103/PhysRevD.82.123535 [arXiv:1008.1231 [gr-qc]].



- [16] A. Bernal and T. Matos, AIP Conf. Proc. **758**, 161 (2005). doi:10.1063/1.1900516
- [17] S. Dodelson and L. M. Widrow, Phys. Rev. Lett. **72**, 17 (1994)  
doi:10.1103/PhysRevLett.72.17 [hep-ph/9303287].
- [18] X. D. Shi and G. M. Fuller, Phys. Rev. Lett. **82**, 2832 (1999)  
doi:10.1103/PhysRevLett.82.2832 [astro-ph/9810076].
- [19] S. Dodelson, A. Melchiorri and A. Slosar, Phys. Rev. Lett. **97**, 041301 (2006)  
doi:10.1103/PhysRevLett.97.041301 [astro-ph/0511500].
- [20] A. Boyarsky, M. Drewes, T. Lasserre, S. Mertens and O. Ruchayskiy,  
arXiv:1807.07938 [hep-ph].
- [21] B. Dasgupta and J. Kopp, Phys. Rev. Lett. **112**, no. 3, 031803 (2014)  
doi:10.1103/PhysRevLett.112.031803 [arXiv:1310.6337 [hep-ph]].
- [22] N. Aghanim *et al.* [Planck Collaboration], arXiv:1807.06209 [astro-ph.CO].
- [23] J. F. Navarro, C. S. Frenk and S. D. M. White, Astrophys. J. **490**, 493 (1997)  
doi:10.1086/304888 [astro-ph/9611107].
- [24] W. J. G. de Blok, Advances in Astronomy 2010 (2010),  
[arXiv:0910.3538[astro-ph.CO]].
- [25] A. A. Klypin, A. V. Kravtsov, O. Valenzuela and F. Prada, Astrophys. J. **522**, 82  
(1999) doi:10.1086/307643 [astro-ph/9901240].
- [26] M. Boylan-Kolchin, J. S. Bullock and M. Kaplinghat, Mon. Not. Roy. Astron. Soc.  
**415**, L40 (2011) doi:10.1111/j.1745-3933.2011.01074.x [arXiv:1103.0007  
[astro-ph.CO]].
- [27] E. Aprile *et al.* [XENON Collaboration], Phys. Rev. Lett. **121**, no. 11, 111302 (2018)  
doi:10.1103/PhysRevLett.121.111302 [arXiv:1805.12562 [astro-ph.CO]].
- [28] A. Boveia and C. Doglioni, Ann. Rev. Nucl. Part. Sci. **68**, 429 (2018)  
doi:10.1146/annurev-nucl-101917-021008 [arXiv:1810.12238 [hep-ex]].
- [29] J. Ipser and P. Sikivie, Phys. Rev. Lett. **50**, 925 (1983).  
doi:10.1103/PhysRevLett.50.925
- [30] P. A. R. Ade *et al.* [Planck Collaboration], Astron. Astrophys. **571**, A16 (2014)  
doi:10.1051/0004-6361/201321591 [arXiv:1303.5076 [astro-ph.CO]].
- [31] C. Destri, H. J. de Vega and N. G. Sanchez, New Astron. **22**, 39 (2013)  
doi:10.1016/j.newast.2012.12.003 [arXiv:1204.3090 [astro-ph.CO]].
- [32] C. Destri, H. J. de Vega and N. G. Sanchez, Astropart. Phys. **46**, 14 (2013)  
doi:10.1016/j.astropartphys.2013.04.004 [arXiv:1301.1864 [astro-ph.CO]].

- [33] V. Domcke and A. Urbano, *JCAP* **1501**, no. 01, 002 (2015)  
doi:10.1088/1475-7516/2015/01/002 [arXiv:1409.3167 [hep-ph]].
- [34] L. Randall, J. Scholtz and J. Unwin, *Mon. Not. Roy. Astron. Soc.* **467**, no. 2, 1515 (2017) doi:10.1093/mnras/stx161 [arXiv:1611.04590 [astro-ph.GA]].
- [35] Y. Sofue, *Publ. Astron. Soc. Jap.* **65**, 118 (2013) doi:10.1093/pasj/65.6.118 [arXiv:1307.8241 [astro-ph.GA]].
- [36] L. D. Landau and E. M. Lifshitz,
- [37] G. Narain, J. Schaffner-Bielich and I. N. Mishustin, *Phys. Rev. D* **74**, 063003 (2006) doi:10.1103/PhysRevD.74.063003 [astro-ph/0605724].
- [38] R. Ibata, G. F. Lewis, M. Irwin, E. Totten and T. R. Quinn, *Astrophys. J.* **551**, 294 (2001) doi:10.1086/320060 [astro-ph/0004011].
- [39] A. M. Ghez *et al.*, *Astrophys. J.* **689**, 1044 (2008) doi:10.1086/592738 [arXiv:0808.2870 [astro-ph]].
- [40] J. Barranco, A. Bernal and D. Nunez, *Mon. Not. Roy. Astron. Soc.* **449**, no. 1, 403 (2015) doi:10.1093/mnras/stv302 [arXiv:1301.6785 [astro-ph.CO]].
- [41] P. Gondolo and J. Silk, *Phys. Rev. Lett.* **83**, 1719 (1999) doi:10.1103/PhysRevLett.83.1719 [astro-ph/9906391].
- [42] S. Riemer-Sørensen, *Astron. Astrophys.* **590**, A71 (2016) doi:10.1051/0004-6361/201527278 [arXiv:1405.7943 [astro-ph.CO]].
- [43] B. Balick and R. L. Brown, *Astrophys. J.* **194**, 265 (1974).
- [44] S. Markoff, H. Falcke, F. Yuan and P. L. Biermann, *Astron. Astrophys.* **379**, L13 (2001) doi:10.1051/0004-6361:20011346 [astro-ph/0109081].
- [45] J. H. Zhao, K. H. Young, R. M. Herrnstein, P. T. P. Ho, T. Tsutsumi, K. Y. Lo, W. M. Goss and G. C. Bower, *Astrophys. J.* **586**, L29 (2003) doi:10.1086/374581 [astro-ph/0302062].
- [46] F. Melia and H. Falcke, *Ann. Rev. Astron. Astrophys.* **39**, 309 (2001) doi:10.1146/annurev.astro.39.1.309 [astro-ph/0106162].
- [47] S. D. Hornstein, A. M. Ghez, A. Tanner, M. Morris, E. E. Becklin and P. Wizinowich, *Astrophys. J.* **577**, L9 (2002) doi:10.1086/344098 [astro-ph/0208239].
- [48] R. Genzel, R. Schodel, T. Ott, A. Eckart, T. Alexander, F. Lacombe, D. Rouan and B. Aschenbach, *Nature* **425**, 934 (2003) doi:10.1038/nature02065 [astro-ph/0310821].
- [49] F. Yuan, E. Quataert and R. Narayan, *Astrophys. J.* **598**, 301 (2003) doi:10.1086/378716 [astro-ph/0304125].

- [50] D. H. Weinberg, J. S. Bullock, F. Governato, R. Kuzio de Naray and A. H. G. Peter, Proc. Nat. Acad. Sci. **112**, 12249 (2015) doi:10.1073/pnas.1308716112 [arXiv:1306.0913 [astro-ph.CO]].
- [51] D. N. Spergel and P. J. Steinhardt, Phys. Rev. Lett. **84**, 3760 (2000) doi:10.1103/PhysRevLett.84.3760 [astro-ph/9909386].
- [52] F. Governato *et al.*, Mon. Not. Roy. Astron. Soc. **422**, 1231 (2012) doi:10.1111/j.1365-2966.2012.20696.x [arXiv:1202.0554 [astro-ph.CO]].
- [53] F. Donato *et al.*, Mon. Not. Roy. Astron. Soc. **397**, 1169 (2009) doi:10.1111/j.1365-2966.2009.15004.x [arXiv:0904.4054 [astro-ph.CO]].
- [54] G. Gentile, B. Famaey, H. Zhao and P. Salucci, Nature **461**, 627 (2009) doi:10.1038/nature08437 [arXiv:0909.5203 [astro-ph.CO]].